1-1-2020

Magnetic field dependence of the martensitic transition and magnetocaloric effects in Ni49BiMn35In15

Anil Aryal
Southern Illinois University Carbondale

Igor Dubenko
Southern Illinois University Carbondale

Saikat Talapatra
Southern Illinois University Carbondale

Alexander Granovsky
Lomonosov Moscow State University

Erkki Lähderanta
LUT University

See next page for additional authors

Recommended Citation

Aryal, A., Dubenko, I., Talapatra, S., Granovsky, A., Lähderanta, E., Stadler, S., & Ali, N. (2020). Magnetic field dependence of the martensitic transition and magnetocaloric effects in Ni49BiMn35In15. *AIP Advances, 10* (1) https://doi.org/10.1063/1.5130405

AIP Advances

Magnetic field dependence of the martensitic transition and magnetocaloric effects in $Ni_{49}BiMn_{35}In_{15}$

Cite as: AIP Advances **10**, 015138 (2020); https://doi.org/10.1063/1.5130405
Submitted: 14 October 2019 • Accepted: 03 January 2020 • Published Online: 17 January 2020

Anil Aryal, Igor Dubenko, Saikat Talapatra, et al.

Magnetic field dependence of the martensitic transition and magnetocaloric effects in $Ni_{49}BiMn_{35}In_{15}$

Cite as: AIP Advances 10, 015138 (2020); doi: 10.1063/1.5130405
Presented: 7 November 2019 • Submitted: 14 October 2019 •
Accepted: 3 January 2020 • Published Online: 17 January 2020

Anil Aryal,[1,a)] Igor Dubenko,[1] Saikat Talapatra,[1] Alexander Granovsky,[2] Erkki Lähderanta,[3] Shane Stadler,[4] and Naushad Ali[1]

AFFILIATIONS

[1]Physics Department, Southern Illinois University, Carbondale, Illinois 62901, USA
[2]Faculty of Physics, Lomonosov Moscow State University, Moscow 119991 Russia
[3]Department of Physics, Lappeenranta University of Technology, Lappeenranta 53851, Finland
[4]Department of Physics and Astronomy, Louisiana State University, Baton Rouge, Louisiana 70803, USA

Note: This paper was presented at the 64th Annual Conference on Magnetism and Magnetic Materials.
[a)]**Corresponding author. Email address:** aryalanil@siu.edu (Anil Aryal).

ABSTRACT

The structural, magnetic, and magnetocaloric properties of the Bi-doped Heusler alloy $Ni_{49}BiMn_{35}In_{15}$ have been investigated using room temperature X-ray diffraction (XRD) and magnetization measurements in a temperature interval of 5-400 K. The alloy at room temperature was found to be in a mixture of a high temperature austenite phase (AP) and a low temperature martensite phase (MP). A drastic shift in the martensitic transition temperature at the rate of 16 K/T from 197 K to lower temperatures was observed. A kinetic arrest phenomenon of the AP was observed in the magnetization and electrical resistivity measurements during field-cooled (FC) measurements at 5T. A metamagnetic behavior characterized by a jump in magnetization in the isothermal $M(H)$ curves near T_M was observed. The maximum value of the magnetic entropy change and refrigerant capacity at Curie temperature were found to be 5.5 $Jkg^{-1}K^{-1}$ and 312 Jkg^{-1} for $\mu_o\Delta H$ = 5T, respectively. A large magnetoresistance value of -56% was found near the martensitic transition.

I. INTRODUCTION

The off-stoichiometric Ni-Mn-In Heusler alloys (with composition near $Ni_{50}Mn_{35}In_{15}$) undergo a diffusionless martensitic phase transition from a cubic to a tetragonal or orthorhombic crystal structure near room temperature. The alloy is ferromagnetic at low temperature (i.e., in the martensite phase (MP)) and undergoes a magnetic transition to a low magnetic (antiferromagnetic or paramagnetic) state at the Curie temperature of the martensitic phase (T_{CM}). A first-order magnetostructural phase transition (MST) from a low magnetic state of the MP to a ferromagnetic state of the austenite phase (AP) at T_M, followed by a magnetic transition of second order (SOT) at T_C, has been observed in these compounds.[1–4] As a result of the first-order MST, the $Ni_{50}Mn_{35-x}In_x$ systems show diverse and unique magnetoresponsive properties such as magnetic shape memory effects, exchange bias, Hall effects, large magnetoresistance, and large normal and inverse magnetocaloric effects.[5–7]

However, these intriguing functional properties related to the MST are extremely sensitive to factors such as chemical composition, doping, conduction electron concentration (e/a), interatomic Mn-Mn distance, fabrication process, thermal annealing, applied magnetic field, and pressure.[1] These factors can affect the phase transitions and the related phenomena in NiMn-based alloys.[8]

In our previous work we reported the effects of the partial substitution of Bi for In on the phase transitions and magnetocaloric properties of $Ni_{50}Mn_{35}In_{15-x}Bi_x$ (x = 0, 0.25, 0.5, 1, 1.5) Heusler alloys.[9] In this work we doped Bi in the Ni sites in $Ni_{49}BiMn_{35}In_{15}$

and studied its influence on the structural, magnetic, and magneto-transport properties. The magnetic field dependence of martensitic transition and the kinetic arrest phenomena of the austenite phase during cooling in the presence of an external magnetic field of 5 T is discussed.

II. EXPERIMENT

The bulk $Ni_{49}BiMn_{35}In_{15}$ alloy was prepared by arc-melting (0.6 wt% loss) followed by annealing at 850 °C for 48 h. The crystal structure was studied by powder X-ray diffraction (XRD) using CuK_α radiation at room temperature. The magnetization and electrical resistivity (four probe method) measurements were performed using a SQUID magnetometer in the temperature range of 10-380 K and in magnetic fields up to 5 T. The magnetization measurements were carried out during the zero-field-cooled (ZFC), field-cooled (FC), and field-cooled-heating (FCH) cycles. The details of the sample synthesis and characterization techniques can be found in Refs. 9 and 10.

III. RESULTS AND DISCUSSIONS

Figure 1 shows the room temperature XRD pattern, which shows that the alloy crystallizes in a mixture of a high temperature austenite phase (AP) and a low temperature martensite phase (MP). Such a mixed phase is commonly observed in NiMn-based Heusler alloys that undergo first-order structural transitions near room temperature.[7,9] The AP can be indexed in cubic structure. The lattice parameter (a) of cubic structure, calculated using the Miller indices (220) of the diffraction peaks, was found to be 5.926 Å.

The FC (open symbols) and FCH (filled symbols) $M(T)$ curves measured at $\mu_o H$ = 0.01 to 5T is shown in Figure 2. A jump-like change in the magnetization and the thermal hysteresis in the FC and FCH curves (upto 4 T) indicate a first-order martensitic

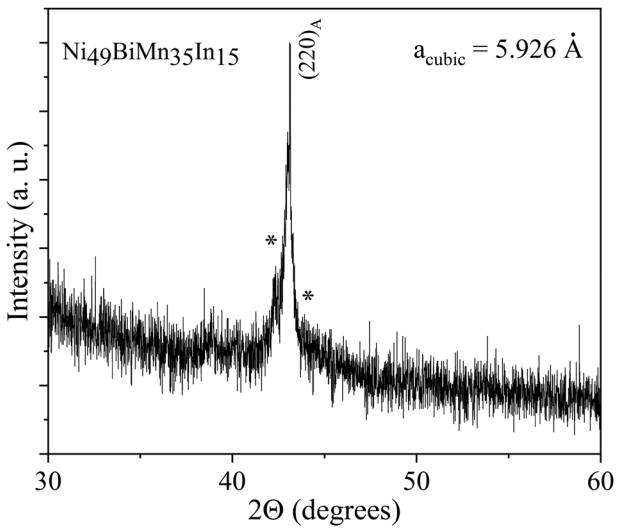

FIG. 1. Powder XRD pattern of $Ni_{49}BiMn_{35}In_{15}$ at room temperature. The low temperature MP are denoted by an asterisk "⁎".

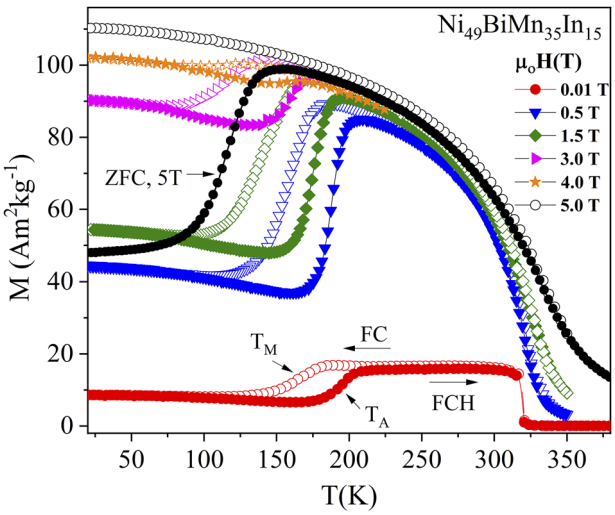

FIG. 2. Magnetization M(T) curves of $Ni_{49}BiMn_{35}In_{15}$ measured at $\mu_o H$ = 0.01 to 5T.

transition (FOT) in this alloy. The direct and reverse martensitic transition temperatures are denoted by T_M and T_A, respectively, in the Figure. A FOT from a ferromagnetic MP to a ferromagnetic AP, and a second-order transition (SOT) from a ferromagnetic AP to a paramagnetic AP (at T_C), were observed on heating at applied magnetic fields up to 4T.

A magnetic field dependence of the martensitic transition was observed in this system. A drastic shift in T_A from 197 K to lower temperatures with applied magnetic field at the rate of ~ 16 K/T was observed (see Fig. S1, ZFC $M(T)$ curves). It is interesting to note that the magnetization at low temperatures below T_M increased with increasing magnetic field. At $\mu_o H$ = 5T, no martensitic transition in the FC curve was observed, which suggests a kinetic arrest of the austenite phase. Similar phenomena have also been reported in other NiMn-based Heusler alloys.[11–17]

In order to confirm the kinetic arrest of the AP in this system, we performed cyclic measurement of the magnetization as follows: (1) first the sample was cooled from 380 K to 10 K in zero field and the ZFC magnetization isotherm was measured up to 5 T; (2) keeping the field at 5 T, the FC $M(T)$ curve was measured from 380 to 10 K; (3) FC $M(\mu_o H)$ isotherms at 10 K were measured from 5 T to 0 T; (4) finally, $M(T)$ measurements were made during heating (FCH) and cooling (FCC) cycles at 0.01T.

As shown in Figure 3, depending upon the cooling protocols, ZFC and FC (at 5T), two ground states characterized by different magnetization values of 40 and 110 Am^2kg^{-1} were found to stabilize at 10 K. Based on the magnetization data, the phases were identified as ferromagnetic AP (110 Am^2kg^{-1}, FC) and MP (40 Am^2kg^{-1}, ZFC), respectively, which confirms the kinetic arrest of the AP in this system by application of $\mu_o H$ = 5T during FC. Note that in FCH $M(T)$ curve at 0.01T, a transition at temperature (T_t) = 25 K appears, which may be related to the transition from the arrested AP to MP.

From the ZFC, FC, and FCH magnetization data (Figure 2 and Figure S1), a magnetic field dependent phase diagram of

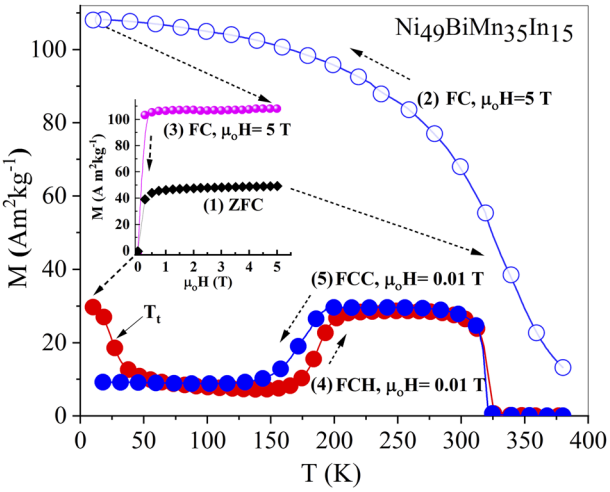

FIG. 3. Isofield magnetization M(T) and isothermal M($\mu_o H$) curves measured under cyclic heating and cooling protocols.

the transition temperatures in this system has been plotted (see Figure 4(a)). As can be seen, the T_C remained almost constant, whereas the martensitic transition temperatures (T_A and T_M) decreased linearly with increasing field. For $\mu_o H$ < 4 T, three types of phase transitions from FM MP to FM AP followed by PM AP exist. Above the critical field $\mu_o H$ = 4 T, two different states, FM MP and FM AP (arrested), occurred depending on the measurement protocols.

A metamagnetic behavior characterized by a jump in magnetization at a critical field ($\mu_o H_C$) in the isothermal $M(\mu_o H)$ curves near the martensitic transition temperature was observed as shown in Figure 4(b). The $\mu_o H_C$ of the metamagnetic transition decreased to lower values with increasing temperature. Based on the magnetization values, it can be identified as a field-induced transition from a FM martensite to a FM austenite phase. At temperatures above the T_C the magnetization showed a linear behavior with the applied field due to FM to PM transition of AP (see Figure S2).

Figure 4(c) shows the magnetic entropy changes $-\Delta S_M$ (T) curves for a magnetic field change of $\mu_o \Delta H$ = 5T. ΔS_M (T) was calculated from the isothermal $M(\mu_o H)$ curves (see Fig. 4(b) and S2) using the Maxwell relation, $\Delta S_M = \int_0^{\mu_o H} \left(\frac{\partial M}{\partial T}\right)_{\mu_o H} d(\mu_o H)$.[18] Both direct and inverse MCE characterized by negative and positive ΔS_M values were observed near T_C and T_M, respectively. A maximum $-\Delta S_M$ of about - 4.5 (at T_M ~ 175 K) and 5.5 Jkg^{-1} K^{-1} (at T_C ~ 325 K) were found for $\mu_o \Delta H$ = 5T. Even though ΔS_M is small, the width of the ΔS_M (T) curve extends over a wide temperature range, which improves the refrigerant capacity (RC). The maximum RC values of 238 and 312 J kg^{-1} at the T_M and T_C were found at 5 T. The obtained RC value of 312 J kg^{-1} at the SOT is nearly double that of those reported for the $Ni_{50}Mn_{35}In_{1-x}Bi_x$ system in our previous work (RC = 165 J kg^{-1} for x = 0.5 at 5 T) and is about 76% of the benchmark Gd (410 J kg^{-1}).[9,18] Because of the irreversible nature of the FOT, the overall value of

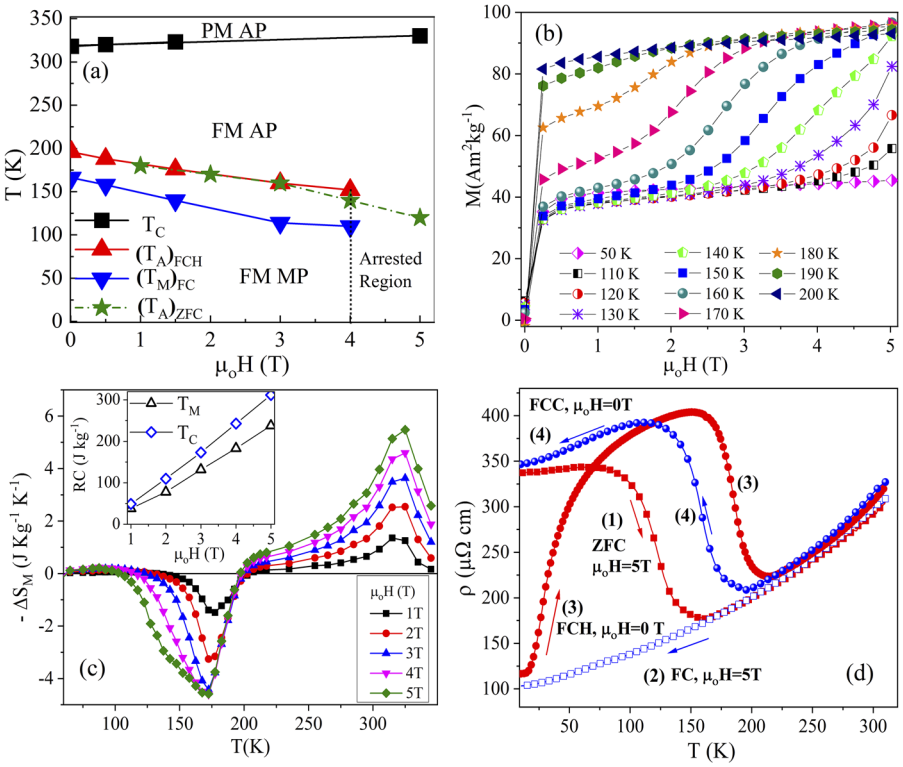

FIG. 4. (a) Magnetic field dependent phase diagram of transition temperatures. (b) Isothermal $M(\mu_o H)$ curves near the martensitic transition temperature. (c) $-\Delta S_M$ (T) curves at $\mu_o \Delta H$ = 5T. Inset: magnetic field dependence of the RC at T_M and T_C. (d) The $\rho(T)$ curves measured under (1) ZFC and (2) FC protocols at $\mu_o H$ = 5 T followed by (3) heating (FCH) and (4) cooling (FCC) cycles at μ_oH= 0 T.

the RC at T_M will be reduced in this system. On the other hand, the magnetic reversibility (with almost zero hysteresis loss) at the SOT resulted in a relatively larger RC value, which could be promising for magnetic refrigeration applications. The magnetic field dependence of the RC at T_M and T_C is shown in the inset of Figure 4(c).

The $\rho(T)$ curves measured under ZFC and FC protocols at 5 T, followed by heating (FCH) and cooling (FCC) cycles at μ_oH= 0 T are shown in Figure 4(d). The abovementioned $\rho(T)$ curves are denoted by the numbers (1), (2), (3), and (4), respectively in the figure. A sharp jump in the resistivity near the martensitic transition temperature was observed in the curves (1), (3), and (4), a behavior typical for NiMn-based Heusler alloys.[1,9,10,19] An irreversibility in the ZFC and FC curves at 5T was observed which can be attributed to the kinetic arrest of the austenite phase during field cooling. As can be seen from the ZFH curve (3), removing the magnetic field does not recover the resistivity value of the martensitic phase (curve (4)) instantly, but the recovery takes place gradually on heating from 10 to 120 K. The resistivity measurements are consistent with the $M(T)$ measurements (see Figure 3). Maximum magnetoresistance (MR) of -56% was calculated from the ZFC ($\mu_o H$ = 5T) and FCH ($\mu_o H$ = 0 T) curves at the martensitic transition.[10]

IV. CONCLUSIONS

The structural, magnetic, magnetocaloric, and transport properties of the Heusler alloy $Ni_{49}BiMn_{35}In_{15}$ have been investigated. Results show: (a) the alloy crystallizes in a mixture of a high temperature AP and a low temperature martensite phase MP at room temperature; (b) an unusual shift in T_A from 197 K to lower temperatures with applied magnetic field at the rate of ~ 16 K/T; (c) a kinetic arrest of the AP during the FC ($\mu_o H$ = 5 T) cycle was observed in the magnetization and electrical resistivity measurements; (d) maximum values of ΔS_M and RC at the SOT were found to be 5.5 $Jkg^{-1}K^{-1}$ and 312 Jkg^{-1} for $\mu_o \Delta H$ = 5T, respectively. Finally, (e) a maximum MR value of -56% was found at the martensitic transition in this alloy.

SUPPLEMENTARY MATERIAL

See supplementary material for additional figures (labeled S1 and S2).

ACKNOWLEDGMENTS

This work was supported by the U.S. Department of Energy (DOE), Office of Science, Basic Energy Sciences (BES) under Award No. DE-FG02-06ER46291 (SIU) and DE-FG02-13ER46946 (LSU), and partly supported by Academy of Finland, grant number 318405.

REFERENCES

[1] I. Dubenko. N. Ali, S. Stadler, A. Zhukov, V. Zhukova, B. Hernando, V. Prida, V. Prudnikov, E. Ganshina, and A. Granovsky, "Magnetic, magnetocaloric, magnetotransport, and magneto optical properties of Ni-Mn-In—Based Heusler alloys: Bulk, ribbons, and microwires," in *Novel Functional Magnetic Materials*, Springer Series in Materials Science, Ed. A. Zhukov, 41–82 (2016).
[2] T. Krenke, M. Acet, E. F. Wassermann, X. Moya, L. Mañosa, and A. Planes, Phys. Rev. B **73**, 174413 (2006).
[3] T. Krenke, E. Duman, M. Acet, E. Eberhard, F. Wassermann, X. Moya, L. Manosa, and A. Planes, Phys. Rev. B **75**, 104414 (2007).
[4] A. P. Kazakov, V. N. Prudnikov, A. B. Granovsky, A. P. Zhukov, J. Gonzalez, I. Dubenko, A. K. Pathak, S. Stadler, and N. Ali, Appl. Phys. Lett. **98**, 131911 (2011).
[5] I. Dubenko, M. Khan, A. K. Pathak, B. R. Gautam, S. Stadler, and N. Ali, J. Magn. Magn. Mat. **321**, 754–757 (2009).
[6] I. Dubenko, T. Samanta, A. Kumar Pathak, A. Kazakov, V. Prudnikov, S. Stadler, A. Granovsky, A. Zhukov, and N. Ali, J. Magn. Mag. Mat. **324**, 3530–3534 (2012).
[7] I. Dubenko, A. Granovsky, E. Lahderanta, M. Kashirin, V. Makagonov, A. Aryal, A. Quetz, S. Pandey, I. Rodionov, T. Samanta, S. Stadler, D. Mazumdar, and N. Ali, J. Magn. Magn. Mater. **401**, 1145–1149 (2016).
[8] I. Dubenko, A. Quetz, S. Pandey, A. Aryal, M. Eubank, I. Rodionov, V. Prudnikov, A. Granovsky, E. Lahderanta, T. Samanta, A. Saleheen, S. Stadler, and N. Ali, J. Magn. Magn. Mater. **383**, 186–189 (2015).
[9] A. Aryal, A. Quetz, S. Pandey, I. Dubenko, S. Stadler, and N. Ali, AIP Advances **8**, 056409 (2017).
[10] A. Aryal, S. Pandey, I. Dubenko, D. Mazumdar, S. Stadler, and N. Ali, IEEE Transactions on Magnetics **55**, 1 (2018).
[11] Y. Koshkid'ko, S. Pandey, A. Quetz, A. Aryal, I. Dubenko, J. Cwik, E. Dilmieva, A. Granovsky, E. Lähderanta, S. Stadler, and N. Ali, J. Magn. Magn. Mater. **459**, 98–101 (2017).
[12] W. Ito, K. Ito, R. Y. Umetsu, R. Kainuma, K. Koyama, K. Watanabe, A. Fujita, K. Oikawa, K. Ishida, and T. Kanomata, Appl. Phys. Lett. **92**, 021908 (2008).
[13] S. Kustov, M. L. Corro, J. Pons, and E. Cesari, Appl. Phys. Lett. **94**, 191901 (2009).
[14] R. Y. Umetsu, W. Ito, K. Ito, K. Koyama, A. Fujita, K. Oikawa, K. Watan-abe, T. Kanomata, R. Kainuma, and K. Ishida, Scripta Mater. **60**, 25 (2009).
[15] V. K. Sharma, M. K. Chattopadhyay, and S. B. Roy, Phys. Rev. B **76**, 140401(R) (2007).
[16] X. Xu, W. Ito, R. Y. Umetsu, K. Koyama, R. Kainuma, and K. Ishida, Mater. Trans. **51**, 469 (2010).
[17] X. Xu, W. Ito, M. Tokunaga, R. Y. Umetsu, R. Kainuma, and K. Ishida, Mater. Trans. **51**, 1357 (2010).
[18] K. A. Gschneidner, Jr., V. K. Pecharsky, and A. O. Tsokol, Rep. Prog. Phys. **68**, 1479 (2005).
[19] A. Aryal, A. Quetz, S. Pandey, I. Dubenko, S. Stadler, and N. Ali, J. Alloys Compounds **717**, 254–259 (2017).